Characterization of Silkworm Chlorophyll Metabolites as an Active Photosensitizer for Photodynamic Therapy

Renke Dai, Richard Shoemaker, David Farrens, Man Jung Han, Choong Sup Kim, and Pill-Soon Song

J. Nat. Prod., **1992**, 55 (9), 1241-1251• DOI: 10.1021/np50087a010 • Publication Date (Web): 01 July 2004

Journal of Natural Products
Vol. 55, No. 9, pp. 1241-1251, September 1992

CHARACTERIZATION OF SILKWORM CHLOROPHYLL METABOLITES AS AN ACTIVE PHOTOSENSITIZER FOR PHOTODYNAMIC THERAPY

RENKE DAI, RICHARD SHOEMAKER, DAVID FARRENS, MAN JUNG HAN,[1] CHOONG SUP KIM,[2] and PILL-SOON SONG*

Department of Chemistry, University of Nebraska, Lincoln, Nebraska 68588-0304

ABSTRACT.—Silkworm excreta containing chlorophyll metabolites have long been used for their medicinal activities in the Far East. The major chlorophyll derivative (CpD) fraction in the Me_2CO extract from the silkworm excreta exhibits strong photodynamic action on mice and human tumor cells in vitro. The main CpD component was isolated, purified, and subjected to extensive structural and characterization studies to assess its photodynamic therapeutic activity. According to the spectral analyses, the structure of the major unknown CpD was determined to be 10-hydroxypheophytin a [**1**]. The CpD component possessed a high quantum efficiency (50%) for the photosensitized production of singlet molecular oxygen, thus providing a molecular basis for its photodynamic therapeutic efficiency. A further advantage is that the "photooxidation/degradation" product(s) from this CpD retains all the characteristics of a photodynamic sensitizer.

Silkworm excreta have been used as a folk medicinal drug in the Far East for centuries (1–3). Recent studies with mice and human tumor cell lines indicated that an active component (CpD, chlorophyll derivative) isolated from the Me_2CO extract of silkworm excreta exhibited strong potential as a photodynamic therapeutic (PDT) sensitizer (2,3). Photofrin II, a commercial photosensitizer which consists of a mixture of hematoporphyrin derivatives (HpD), has been widely used in the PDT of tumor cells. Some derivatives of chlorophylls have also been shown to exhibit photochemical characteristics that are consistent with anti-cancer PDT drugs (4–7). There are many advantages to using a CpD over HpD, including a higher yield of reactive oxygen such as $^1O_2$ and O_2^- and CpD can be more easily cleansed from tissue after PDT treatments. Moreover, CpD can be excited by light of greater tissue-penetrating longer wavelengths (λ_{CpD}>650 nm; λ_{HpD}=ca. 610 nm) (8).

Recently, Park *et al.* (2) and Lee *et al.* (3) reported that certain CpD fractions from the tlc of silkworm metabolites were effective for PDT for test animals, exhibiting photodynamic killing of ascites tumors in mice as well as human and mouse tumor cells in vitro. These studies show that when a human T-cell lymphoma line (MOLT-4) was used as the target tumor cell and a fresh human peripheral blood lymphocyte (PBL) was used as a control normal cell, the uptake of an unidentified CpD from silkworm excreta by the tumor cell was twice that of HpD. The photodynamic effect of the unidentified CpD upon red light irradiation for 10 min resulted in the complete killing of the tumor cells examined. However, no significant photodynamic killing of tumor cells was observed by HpD under similar conditions. These results showed that an unidentified CpD was superior to HpD as a PDT sensitizer.

In the present study, we isolated and purified an essential CpD component for PDT from silkworm excreta, using tlc, liquid chromatography, and reversed-phase hplc. This highly purified CpD was then subjected to structural analysis methods such as electronic and cd spectroscopy, ms, Ft-ir, and high resolution 1D and 2D nmr. The essential CpD component was determined to be 10-hydroxypheophytin a [**1**]. Its properties as a PDT sensitizer were also characterized. Fischer nomenclature is used in this report.

---

[1]Present address: Department of Applied Chemistry, Ajou University, Suwon, Korea.
[2]Present address: Cheil Foods and Chemicals Co., Ichon, Korea.

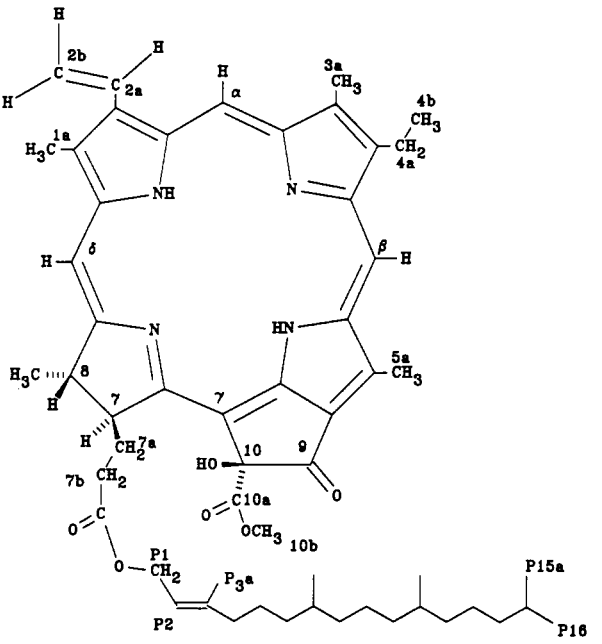

1

RESULTS

OPTICAL PROPERTIES OF CRUDE EXTRACT.—For spectral, photochemical, and structural characterization of the CpD's in silkworm excreta, dry samples from a crude Me_2Co extract were redissolved in Me_2CO. After filtering insoluble materials, the solutions were evaporated under a nitrogen atmosphere to complete dryness. The resulting materials were then dissolved in pure EtOH. Absorbance maxima were shown at 666 and 408 nm. The fourth derivative spectrum resolved peaks at 689 (minor peak), 668, 438, 416, 398, and 376 nm, suggesting that the absorbance spectrum is a composite of more than one visible light-absorbing CpD. The multi-composite nature of the spectrum was further confirmed by fluorescence excitation and emission spectral analysis.

CHROMATOGRAPHIC ANALYSIS.—The tlc results (Figure 1) show that the second major band (from top) in the crude Me_2CO extract of the silkworm feces is unique, compared to the tlc results for Me_2CO extracts from mulberry and spinach leaves. All other major tlc bands seen in Figure 1 can be identified in terms of known reference chlorophylls and carotenoids (data not shown). Moreover, it was shown that the eluate from the second band (band 2) was the major PDT component when tested with mice and human tumor cell lines (2,3). Thus, we decided to characterize this second band component.

When the band 2 eluate from an older tlc plate exposed to fluorescent light was analyzed by reversed-phase hplc, four peaks having different retention times were resolved, with the second peak (P2) being the principal component (Figure 2a).

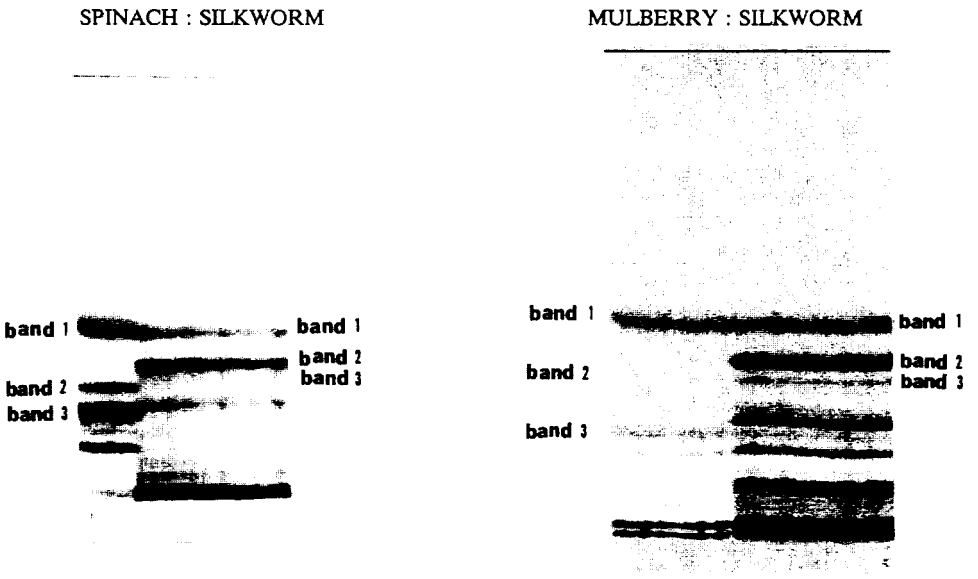

FIGURE 1. Tlc of crude extracts. (Left panel) Comparison between spinach leaves and silkworm excrements. The materials in the first three bands as marked in the spinach part are identified as pheophytin a, chlorophyll a, and chlorophyll b (or their derivatives). (Right panel) Comparison between mulburry leaves and silkworm feces. The materials in the first and third bands from mulberry are the derivatives from chlorophyll a, and that of the second band is from chlorophyll b. The second band from the silkworm extract represents a major metabolite (CpD). The yellow and orange colored bands are due to carotenoids.

However, the band 2 eluate from a freshly purchased tlc plate that was not exposed to light showed P3 as the main component in the hplc profile (Figure 2b). It was subsequently proven that the former (P2) is a protoisomer/photooxidation product of the latter. Moreover, when Si gel liquid chromatography, instead of Si gel tlc, was employed to obtain band 2, the resulting hplc profile (Figure 2c) showed no P2, and only P3 as the main component. Thus, it appears that P2 is an isolation artifact produced by the photochemical isomerization and/or photooxidation of P3. Irradiation of P3 in EtOH did not yield any significant amount of P2.

SPECTROSCOPIC AND PHOTOPHYSICAL CHARACTERIZATION.—The absorbance spectra of P3 showed λ max 666 nm, and that of P2 showed λ max 568 nm. The absorbance spectrum of P2 in EtOH clearly indicated a minor component with an absorbance peak at 688 nm. However, this component disappeared in dry *n*-hexane. It is likely that the 688-nm-absorbing species is attributable to either a P2 dimer or an H-bonded isomeric species. However, the cd spectra of P2 in EtOH and dry *n*-hexane did not show an exciton-like splitting expected from a stacked dimer species; instead, the Q_y band was red-shifted in EtOH. the fact that P2 in EtOH was strongly fluorescent is consistent with the 688-nm species being an H-bonded isomer, since the stacked dimers of chlorophyll derivatives are only very weakly fluorescent. In contrast, the P3 spectrum did not reveal a shoulder/peak at 688 nm in EtOH or dry *n*-hexane.

Photophysical parameters of P3 and P2 determine the upper limit of their efficiency

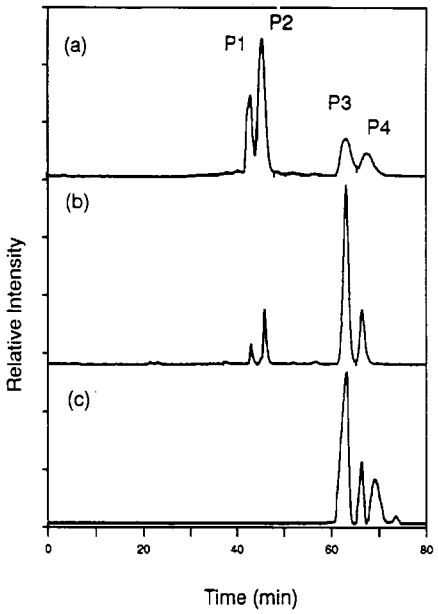

FIGURE 2. Hplc profiles. (a) Tlc band 2 was subjected to reversed-phase hplc, from tlc sheets that were exposed to white light and air. (b) The same material as (a) but with no exposure to white light and no wait before performing hplc after the tlc. (c) Fraction of band 2 from Si gel liquid chromatography was injected into the hplc. All of the above hplc's were performed under the same solvent conditions using the same gradient program.

as PDT photosensitizers. Both steady state and dynamic fluorescence properties of the P2 and P3 compounds were determined to assess their potential as PDT drugs. Chlorophyll a was used as a reference for quantum yield determinations (9), after further purification using reversed-phase hplc. The fluorescence quantum yield (ϕ_x) of an unknown compound can be calculated according to the following relationship:

$$\phi_x=\phi_{chl}\frac{A_{chl}\cdot[\int F(\nu)\,d\nu]_x}{A_x\cdot[\int F(\nu)\,d\nu]_{chl}}$$

where A is absorbance at the exciting wavelength of 620 nm, and $[\int F(\nu)d\nu]$ is the total fluorescence intensity integrated from the emission spectrum plotted in linear energy scale. The quantum yields determined from these calculations are presented in Table 1. From Table 1, P3 is shown to be the weakest emitter. The P3 decay is essentially single exponential, whereas the P2 decay is best described by bi-exponentials ($\chi^2\approx1$), although the second component showed a very small negative amplitude (>2%). Table 1 lists the fluorescence lifetime data. Consistent with the fluorescence quantum yield data, P3 shows the shortest lifetime among the three CpD's measured.

SINGLET OXYGEN PRODUCTION.—One of the most important criteria that determines the ultimate efficiency of a PDT photosensitizer is its ability to generate singlet oxygen via energy transfer from the triplet photosensitizer to molecular oxygen (10). We employed two independent methods to determine the quantum yields of singlet oxygen, as described in the Experimental section. The photooxidation method uses a singlet oxygen trap [1,3-diphenylisobenzofuran (DPBF)] (11,12), and the rate of photooxida-

TABLE 1. Fluorescence Quantum Yield and Lifetime Data.

	Chlorophyll a	1	P2
A (620 nm)	0.0961	0.0933	0.1051
$[\int F(\nu)\, d\nu]_f$	5,353,179	2,021,984	3,989,275
ϕ_f	0.24[a]	0.09	0.16
τ_{exp}[b] (nsec)	5.15	4.12	4.56
SD (nsec)	0.006	0.011	0.008

[a]According to Forster and Livingston (9).

[b]Absorbance of each dye at its red absorbance band λ max was <0.2 for lifetime measurements.

tion of DPBF is followed in terms of decrease in DPBF fluorescence or absorbance to estimate the initial rates of photooxidation of DPBF in the presence of CpD's. The initial DPBF photooxidation rate inversely reflects the initial rate of singlet oxygen production (11,12). As controls, we checked for changes in absorbance/fluorescence emission of DPBF without light or photosensitizers. No significant changes (i.e., photooxidation of DPBF) were observed with either the absence of sensitizers or without irradiation by the helium-neon laser.

A double reciprocal plot of 1/rate vs. 1/[DPBF] yields a maximum initial rate from the reciprocal intercept. The quantum yield of singlet oxygen of chlorophyll a in EtOH ($\phi_{\Delta,x}$ in EtOH) was then calculated from the maximum initial rate, relative to the known singlet oxygen yield of chlorophyll a in CCl_4 as reference ($\phi_{\Delta,chl}=0.57$ in CCl_4) (13) by the equation:

$$\phi_{\Delta,x}=\phi_{\Delta,chl}\frac{A_{chl}\cdot[RATE_{max}]_x}{A_x\cdot[RATE_{max}]_{chl}}$$

where A and x stand for absorbance and unknown sample, respectively. This equation was also used for the quantum yield calculation for unknown samples in EtOH. The results from both methods are presented in Table 2. Both P3 and P2 are capable of generating singlet oxygen with equal or higher efficiency than chlorophyll a. The singlet oxygen quantum yields obtained by the direct emission method are in excellent agreement with the data from the chemical trap (DPBF photooxidation) method, indicating that the photooxidation of DPBF proceeded predominantly via a Type II singlet oxygen route.

TABLE 2. Singlet Oxygen Yields (ϕ_Δ) Determined by the Relative Photooxidation of DPBF (I) and Direct Luminescence Method (II).

Method	Item	Chlorophyll a	1	P2
I	ϕ_Δ of $(DPBF)_{ox}$	0.44[a]	0.50	0.52
	Relative I_Δ	1.00	1.01 ± 0.05	1.09 ± 0.04
II	$\tau_{\Delta(\mu sec)}$	30.5 ± 0.8	31.6 ± 0.4	28.9 ± 1.1
	Relative ϕ_Δ	1.00	1.05 ± 0.06	1.16 ± 0.05
	ϕ_Δ	0.44[a]	0.46 ± 0.03	0.51 ± 0.02

[a]This is the average value by comparison of chlorophyll a in EtOH and CCl_4 from absorbance method and emission method (graph not shown).

STRUCTURE ELUCIDATION.—To elucidate the structure of the major CpD component (P3), hrfabms and nmr analyses were performed. The mol wt of P3 determined by hrfabms measurements was *m/z* 886.5597, which yielded the elemental composition of $C_{54}H_{74}O_6N_4$ (calcd 886.5608). A tandem ms analysis of the fragmentation pattern for this molecular ion showed a major fragment of *m/z* 608, which corresponds to a dephytylated molecular ion of CpD (14). From the ms data, we deduced a monooxygenated pheophytin-a-like structure for P3.

1D and 2D ^{1}H-nmr experiments, in addition to ^{13}C nmr, were performed on the P3 sample, and the single pulse (1D) ^{1}H-nmr data were compared to that of a sample of highly purified chlorophyll a as a reference, with the spectral assignments listed in Table 3. Two-dimensional correlation spectroscopy (COSY) was used to confirm assignments of all hydrogens involved in homonuclear *J* coupling. Assignments of uncoupled protons (such as α, β, and δ) were checked against literature data of chlorophyll a in THF-d_8 (15). P3 spectra were acquired in both THF-d_8 and $CDCl_3$ to ensure that no unexpected solvent effects were overlooked.

TABLE 3. Proton Chemical Shifts (δ, ppm) of Chlorophyll a and **1**.[a]

Proton	Chlorophyll a	**1**
H-α	9.61	9.75
H-β	9.47	9.59
H-δ	8.63	8.75
H-2a	8.00	8.03
H-2b$_t$	6.29	6.31
H-2b$_c$	6.20	6.22
H/OH-10	6.27	5.57
P2	5.14	5.22
P1	4.49	4.56
H-8	4.44	4.53
H-7	4.24	4.20
H-4a	3.87	3.77
H-10b	3.87	3.76
H-3a	3.70	3.60
H-1a	3.41	3.44
H-5a	3.26	3.29
H-7a$_1$	2.64	2.95
H-7b$_1$	2.48	2.56
H-7a$_2$	2.34	2.26
H-7b$_2$	2.34	2.26
P4	1.88	1.91
H-4b	1.81	1.70
P3a	1.70	1.61
H-8a	1.57	1.60
P15	1.49	1.49
P(CH$_2$)$_8$	1.24	1.24
P15a and P16	0.84	0.84
P7 and P11	0.78	0.79

[a]In $CDCl_3$.
[b]Based on the Fischer numbering system.

The spectra of the P3 compound clearly indicated a structure identical to that of chlorophyll a, with the exception of the N-H protons inside the porphyrin and an X-H proton at position 10 (where X is an unknown element). In chlorophyll a (in $CDCl_3$), the

H-10 is found at 6.27 ppm; however, this signal is absent in the P3 spectrum, and another appears at 5.57 ppm. D_2O exchange experiments confirmed that the peak at 5.57 ppm is highly exchangeable; thus, it is most likely an O-H moiety. The peak at 5.57 ppm disappeared immediately upon addition of one drop of D_2O. This is in contrast to the H-10 proton of chlorophyll a which has been shown to undergo proton exchange with a time constant on the order of an hour (16). Further evidence that the peak at 5.57 is OH in nature can be found by comparison of the spectra acquired in $CDCl_3$ vs. THF-d_8. The peaks between the two experiments are comparable, except for the position-10 peak which shifts from 5.57 ppm to 7.01 ppm. The literature value for the H-10 proton in THF-d_8 is 6.18 ppm (15) (less than 0.1 ppm different than what we observed in $CDCl_3$ (6.27 ppm). Such a dramatic solvent effect on a single resonance is indicative of a specific interaction of that moiety with the solvent, in this case, THF-d_8. It is well known that hydrogen bonding causes a downfield shift of one to two ppm for an OH proton (17).

Variable temperature experiments were performed to investigate the dynamic nature of the system and to explore the possibility of intra-molecular hydrogen bonding of the OH proton at position 10 with the carbonyl oxygen at 10a and/or 7c. At room temperature, it is expected that the proton will be in fast-exchange between the oxygen atoms; however, lowering the temperature should cause a clear shift in resonance position and a peak broadening as an intermediate exchange regime is encountered. The proton resonance in question shifts and broadens with lower temperature, which supports the 10-OH proton being involved in a fast chemicial exchange at room temperature. Interestingly, the "meso" protons (α, β, and δ) broaden steadily into the baseline with lowering temperature. Due to their proximity to the tremendous deshielding effects of the porphyrin ring currents, these protons are in an extremely anisotropic shielding environment and at 500 MHz would normally be expected to drop out of the extreme-narrowing regime as the temperature is dropped. No other ^{1}H-nmr signals are significantly altered by the temperature change.

It is important to point out that one alternative explanation for all of the above results would be an enol tautomer at positions, 9,10. This could account for the OH signal, the loss of the signal from H-10 upon D_2O exchange, and the variable temperature results. However, we feel this explanation can be discounted, because the ^{13}C-nmr results clearly show a ketone resonance at position 9 at 191.8 ppm. Otherwise, the ^{13}C-nmr results agree well with literature data on similar compounds, such as bacteriochlorophyllide c derivatives (18), with one exception. The ^{13}C resonance at 89.0 ppm has no counterpart in the above reference compounds and has been tentatively assigned to C-10. This assignment is substantiated by DEPT experiments which unambiguously show the CH_n multiplicity. Sensitivity considerations precluded our performing comprehensive heteronuclear, multi-dimensional techniques which would allow unambiguous assignment of all C-13 signals.

The 2D-NOESY nmr analysis indicated no evidence for a P3 dimer/oligomer in EtOH at room temperature (data not shown). The Ft-ir spectrum of P3 showed a C-OH stretching vibration at 1052 cm^{-1} [lit. (19) 1000–1260 cm^{-1}; methylvinylcarbinol, 1058 cm^{-1}]. The non-hydrogen-bonded OH stretching at about 3300 cm^{-1} can disappear due to the formation of intramolecular hydrogen bonding (19). As mentioned above, the 10-OH group in P3 has two likely sites of intramolecular hydrogen bonding with the carbonyl oxygens. Combining all of the above-described spectral data, the structure of P3 is concluded to be that of a 10-hydroxypheophytin a [**1**]. This assignment was further supported by comparing the absorbance spectra of P3 and 10-hydroxypheophytin a recently synthesized by Professor H. Scheer (private communication, 1991).

DISCUSSION

Rabinowitch has suggested that a "lone" hydrogen atom at position 10 of chlorophylls can readily be oxidized (20), and thus 10-methoxychlorophylls can be generated by adding quinone and MeOH to chlorophylls in vitro. 10-Hydroxychlorophylls as allomerized products have also been suggested to form during air oxidation of chlorophylls. Similar blue-green chlorophyll products can be produced by enzymatic oxidation of chlorophylls (21). Pennington et al. (22) have identified one of the enzymatically oxygenated chlorophylls as 10-hydroxychlorophyll. Heating and/or organic solvents affected the generation of 10-hydroxychlorophyll derivatives in vitro, and these were referred to as "changed" CpD's (23). Identical "changed" CpD's could also be derived from purified chlorophylls a and b nonenzymatically. These early studies and more recent reports, therefore, indicate that hydroxylation of chlorophylls occurs readily in vitro (4,21–26). However, the fact that 10-hydroxypheophytin a [1] is the unique metabolic product (P3) of silkworm and/or its digestive tract microbes has not previously been reported in the literature.

Because the Me_2CO extracts of mulberry and spinach leaves showed virtually no trace of band 2 on tlc, and no **1** or P2 by hplc under identical sample treatment conditions, we conclude that **1** is an enzymatic metabolite produced during the metabolism of chlorophyll a in silkworms. The band 2 and **1** were also resolved by Si gel liquid chromatography, indicating that 10-hydroxylation of chlorophyll a, which might be formed artificially by tlc procedures (25), is not responsible for the formation of **1** in the Me_2CO extract from silkworm excreta. How de-magnesium and hydroxylation reactions of chlorophyll a occur in vivo remains to be investigated.

The concentration of **1** in freeze-dried crude extract of the silkworm excreta was estimated to be at least 0.7% by weight, assuming a 100% recovery at each of step of the chromatography-elution procedure [average of three determinations based on a molar extinction coefficient (ϵ) of 49,000 at 666 nm]. In terms of absorbance, the compound **1** absorbance accounts for 7% of the total absorbance at 666 nm of the crude extract.

The mechanism of the **1**→P2 phototransformation/photooxidation cannot be elucidated without examination of the structure of P2. The fact that P2 fluoresces more strongly than **1** and that absorbance at approximately 500 nm is essentially lacking in the absorbance spectrum of P2, compared to that of **1**, is consistent with a metal-chelated 10-hydroxypheophytin a isomer for the P2 structure (private communication, H. Scheer, 1991). It is significant that P2 retains/improves the PDT efficiency criteria of **1**, in terms of optical and photophysical characteristics (Table 1) and singlet oxygen yield (Table 2). For the discussion hereafter, we will refer these 10-hydroxypheophytin derivatives as silkworm CpD.

HpD's are currently the major sensitizers used for PDT in clinical trials. Silkworm CpD's appear to offer an excellent alternative to HpD. For example, silkworm CpD's absorb at longer wavelength and more strongly than HpD; thus the laser light wavelength used has greater tissue penetration of PDT light. Efficiency of singlet oxygen production is significantly higher with silkworm CpD (50%, Table 2) than with HpD [lit. (27) 35%]. More importantly, silkworm CpD's exhibit a greater affinity for tumor tissue than HpD's, and their retention times in test animals are considerably shorter than that of HpD (2,3), thus minimizing undesirable cytotoxic effects in vivo. Tests both in a human tumor cell line and in mice showed that the PDT efficacy of silkworm CpD is at least equal to or greater than that of HpD. These observations support the notion that silkworm CpD's, mainly 10-hydroxypheophytin a, are potentially an effective photosensitizer for use in PDT clinical applications.

CONCLUSIONS

The structure of the major component of silkworm CpD was found to be 10-hydroxypheophytin a [**1**]. 10-Hydroxypheophytin a offers an excellent potential as a PDT sensitizer. Since its photoisomerization/photooxidation product, P2, retains or exceeds photophysical and photochemical characteristics of **1** as a PDT photosensitizing drug, silkworm CpD circumvents the photolability problem of other sensitizers such as HpD. Furthermore, since P2 appears to be formed photochemically only on the Si gel matrix and not in solution, it is unlikely that P2 would be formed to any significant extent in vivo. Other advantages include greater light penetration through tissues, stronger PDT effect, low cost, and easy tissue cleansing (2–7). The present conclusion is supported by the recent findings that chlorin derivatives are potentially efficient sensitizers for PDT applications (4–7). However, no studies have been reported on the characterization of 10-hydroxypheophytin a and its photoisomer/photooxidation product as PDT sensitizer drugs.

EXPERIMENTAL

CRUDE EXTRACT PREPARATION.—For isolation and purification of silkworm CpD's, an Me_2CO extraction was used for the present study. Crude extracts from silkworm metabolites (digestive excreta) and mulberry leaves were obtained from Samsung and Cheil Foods & Chemical Company, Korea. Crude extract from spinach leaves was prepared according to a published procedure (28).

TLC OF THE CRUDE EXTRACT.—Plastic tlc sheets of Si gel (20×20 cm) were used (tlc plastic Si gel, Art. 5735, EM Science). For initial tlc development and comparisons (29), the solvent system contained *t*-BuOH–Me_2CO–pentane (5:60:235). All manipulations were performed in the dark or under dim green light.

After development of the crude extract on tlc, the second band (band 2) was carefully cut out and extracted with Me_2CO. The eluate was evaporated under an N_2 stream and stored until hplc purification.

SI GEL LIQUID CHROMATOGRAPHY.—Si gel (70–230 mesh from Sigma Chemical Co., 25 g) was equilibrated in *n*-pentane for 2 h or longer and then degassed using a sonicator (Bransonic 12) for at least 0.5 h. An aspirator was used to degas further for about 10 min. The degassed Si gel was then packed inside a glass tube and allowed to stand overnight to equilibrate. The column height was 10–15 cm with a diameter of 2.5 cm. Before sample loading, the column was washed with two times the column volume of *n*-pentane with a flow rate of 2 ml/min. Approximately 0.05 g of crude extract was dissolved in 1.5 ml Me_2CO–*n*-pentane (1:1). After applying the sample, approximately 1.5-fold the column volume of *n*-pentane was used to elute the column. During this procedure, it was observed that several bands were separated in the column. When the first band nearly stopped migrating, the mobile phase was changed to 5% Me_2CO in pentane (about half a column volume). Finally, 10% Me_2CO in pentane was applied. Only the second elution band was collected. The solvents were evaporated under an N_2 stream and stored until hplc purification.

HPLC PURIFICATION.—An ISCO Model 2350 hplc, a model 2360 gradient programmer, a UV-5 absorbance/flluorescence detector (ISCO, Inc.), and a C-18 dynamax-300Å (1×25 cm) (Rainin Instrument Company, Inc.) were used. Hplc purification was carried out by a method modified from the published procedure for spinach clorophylls (30). Hplc conditions for the purification of the major component in silkworm crude extract were as follows: flow rate 1.7 ml/min; mobile phase 35% MeOH and 65% MeCN; gradient from 80% mobile phase and 20% H_2O to 100% mobile phase for 25 min. Injection volumes of 200 μl of samples having absorbance of about 7.0 at 660 nm (approximately 25 μg) were used.

ABSORPTION AND CD SPECTROSCOPY.—Samples were dissolved in EtOH, and absorbance spectra were measured using an HP 8452 diode array spectrophotometer (Hewlett-Packard) or Shimadzu UV-265 spectrophotometer with microcomputer capabilities. The fourth derivative spectra were recorded on both. CD spectra were measured on a JASCO J-600 CD spectropolarimeter.

FLUORESCENCE QUANTUM YIELD.—Fluorescence emission measurements were performed using an excitation wavelength of 620 nm on an RF-540 spectrofluorophotometer (Shimadzu). The sample concentration was kept below an absorbance about 0.1 at 620 nm in EtOH.

FLUORESCENCE LIFETIME MEASUREMENTS.—Fluorescence decay times were measured by the time-

correlated single photon counting method (31) using a modified Edinburgh Instrument 299T lifetime system that employs a pulsed diode-laser (32). The pulsed diode laser light source (Hamamatsu Photonics PLP-01, 660 nm) was operated at a frequency between 1 and 3 MHz. Fluorescence was detected at 725 nm with slit width of 4 nm at right angles to excitation by a red-sensitive photomultiplier tube (Phillips XP2254B), followed by time-to-amplitude conversion (Ortec 567) and pulse shaping by constant fraction discriminator (Edinburgh CF4000). Count rates were kept below 0.1% (1000 counts/sec) to avoid pile-up. Light intensity of the diode-laser was varied by the use of a linear wedge neutral density filter (Ealing Electro Optics) or aperture attenuation. The negative pulse (approximately 10 nsec) from the trigger-out on the back of the PLP-01 was processed through a constant fraction discriminator to provide better timing signals. Data were first stored on a multi-channel pulse height analyzer (Ortec 5600), and subsequently the data obtained were transferred to a computer. All data analyses were performed by a non-linear least squares reconvolution method (33) using commercially available software (Edinburgh Instrument).

SINGLET OXYGEN YIELD.—*Chemical trap method.*—A 632.8 nm helium-neon laser (20 mW maximum output, Metrologic Instruments, Inc.) was used as an irradiation source to excite the sample solution. A solution of DPBF (recrystallized under N_2 in the dark) in EtOH was prepared immediately before use, and the concentration was checked by using $\epsilon = 22{,}500\ cm^{-1}M^{-1}$ at 420 nm (34). In a closed cuvette containing a total of 2 ml of solution, each sensitizer had almost the same absorbance at 632 nm. O_2 gas presaturated with solvent was used to gently bubble the solution for 20 min, after which a small aliquot of different concentrations of DPBF was mixed with the solution. The decrease in the fluorescence intensity of DPBF at 455 nm in EtOH and 465 nm in CCl_4 was measured as a function of irradiation time to determine initial rates of photooxidation of DPBF, in which the excitation wavelength was 324 nm. In the absorption method, the decrease in the absorbance of DPBF at 412 nm instead of the fluorescence emission was followed. The results from the emission and absorbance methods were essentially identical.

Near-ir phosphorescence method.—To detect singlet oxygen directly, the near-ir phosphorescence was measured. A Q-switched Nd: YAG laser (Quantel, YG-571-C) was operated at 355 nm. Details are described by Rodgers (35). The silkworm CpD and chlorophyll a samples were dissolved in air-saturated EtOD, and sample concentrations were kept almost the same by adjusting the absorbance to about 0.55 at 355 nm. Measurements were performed at the Center for Photochemical Sciences, Bowling Green State University, Ohio.

NMR MEASUREMENTS.—Nmr data were acquired on a General Electric Omega-500 nmr instrument. Samples were prepared by dissolving approximately 1 mg/ml of sample for ^1H and 5 mg/ml for ^{13}C measurements. The 2D COSY spectrum was acquired.

A standard DEPT pulse sequence was applied to elucidate the multiplicities using θ pulses of 90° and 135° with no further ^{13}C spectral editing.

MASS SPECTROMETRY.—A Kratos MS-50 triple-analyzer mass spectrometer of EB/E design was used (Ion Tech, Middlesex, England) (14). For fab/ms/ms tandem mass spectrometric measurements, silkworm CpD in a matrix of 3-NBA was bombarded by a source of 7–8 kV argon atoms accelerated through a potential of 8 kV. The peak resolution of 10,000 was matched to appropriate CsI/glycerol reference ions for accurate mass measurements. Measurements were performed in the Midwest Center for Mass Spectrometry, University of Nebraska–Lincoln.

FT-IR.—Ft-ir spectra were acquired with a Laser Precision RFX-65 Spectrophotometer (Analect Instruments) using Attenuated Total Reflectance sampling with a thallium halide (KRS-5) crystal. Samples were prepared by evaporating 1–2 drops of 2 mg/ml $CHCl_3$ solution on the crystal surface, leaving a thin film in close contact with the KRS-5.

ACKNOWLEDGMENTS

This work was supported by Samsung and Cheil Food & Chemical Co., Korea, and in part by NIH grant GM 36956 and by the U.S. Army Research Office (28748-LS-SM). We thank Professor M.A.J. Rodgers and W. Ford for performing ir luminescence measurements, Dr. Ronald L. Cerny for the ms measurements and Todd Wells for photographing the tlc chromatograms. We thank Professor David Hage, UNL, and Professor Hugo Scheer, University of Munich, for helpful discussions.

LITERATURE CITED

1. Z. Zhang, Z. Hong, and L. Liu, *J. Sichuan Univ., Nat. Sci. Ed.*, **25**, 216 (1988).
2. Y.J. Park, W.Y. Lee, B.S. Hahn, M.J. Han, J.K. Roh, and B.S. Kim, *J. Korean Cancer Res. Assoc.*, **21**, 1 (1989).

3. W.Y. Lee, J.H. Park, B.S. Kim, M.J. Han, and B.S. Hahn, *Yonsei Med. J.*, **31**(3), 225 (1990).
4. H. Endo, H. Hosoya, T. Koyama, and M. Ichioka, *Agric. Biol. Chem.*, **46**, 2183 (1982).
5. E.M. Beems, T.M.A.R. Dubbelman, J. Lugtenburg, J.A. Van Best, M.F.M.A. Smeets, and J.P.J. Boegheim, *Photochem. Photobiol.*, **46**(5), 639 (1987).
6. G. Schermann, A. Volcker, K. Seikel, R. Schmidt, H.D. Brauer, and F.P. Montforts, *Photochem. Photobiol.*, **51**, 45 (1990).
7. R.K. Pandey, D.A. Bellnier, K.M. Smith, and T. Dougherty, *Photochem. Photobiol.*, **53**, 65 (1991).
8. A.E. Profio and D.R. Doiron, *Photochem. Photobiol.*, **46**(5), 591 (1987).
9. L.S. Forster and R. Livingston, *J. Chem. Phys.*, **20**, 1315 (1952).
10. J.D. Spikes, in: "The Science of Photobiology." Ed. by K.C. Smith, Plenum Press, New York, 1989, pp. 79–110.
11. I.B.C. Matheson, J. Lee, B.S. Yamanashi, and M.L. Wolbarsht, *J. Am. Chem. Soc.*, **96**, 3343 (1974).
12. A. Singh, E.R. McIntyre, and G.W. Koroll, *Photochem. Photobiol.*, **28**, 595 (1978).
13. A.A. Krasnovsky Jr., K.V. Neverov, S.Y. Egorov, B. Roeder, and T. Levald, *J. Photochem. Photobiol.*, **5**, 245 (1990).
14. R.P. Grese, R.L. Cerny, M.L. Gross, and M. Senge, *J. Am. Soc. Mass Spectrom.*, **1**, 72 (1990).
15. S. Lotjonen, T.J. Michalski, J.R. Norris, and P.H. Hynninen, *Magn. Reson. Chem.*, **25**, 670 (1987).
16. R.C. Dougherty, H.H. Strain, and J.J. Katz, *J. Am. Chem. Soc.*, **87**, 104 (1965).
17. R.M. Silverstein, G.C. Bassler, and T.C. Morrill, "Spectrometric Identification of Organic Compounds," 5th ed., John Wiley and Sons, New York, 1991, p. 183.
18. F. Fages, N. Griebenow, K. Griebenow, A.R. Holzwarth, and K. Schaffner, *J. Chem. Soc., Perkin Trans. 1*, 2791 (1990).
19. R.M. Silverstein, G.C. Bassler, and T.C. Morrill, "Spectrometric Identification of Organic Compounds," 5th ed., John Wiley and Sons, New York, 1991, p. 109.
20. E.I. Rabinowitch, "Photosynthesis and Related Processes," Interscience Publishers, New York, 1945, pp. 438–469.
21. H.H. Strain, *J. Am. Food Chem.*, **2**, 1222 (1954).
22. F.C. Pennington, H.H. Strain, W.A. Svec, and J.J. Katz, *J. Am. Chem. Soc.*, **89**, 3875 (1967).
23. M.F. Bacon and M. Holden, *Phytochemistry*, **6**, 193 (1967).
24. D. Dornemann and H. Senger, *Photochem. Photobiol.*, **43**, 573 (1986).
25. M. Senge, D. Dornemann, and H. Senger, *FEBS Lett.*, **234**, 215 (1988).
26. S. Schoch, W. Rudiger, B. Luthy, and P. Matile, *J. Plant Physiol.*, **115**, 85 (1984).
27. W.F. Keir, E.J. Land, A.H. MacLennan, D.J. McGarvey, and T.G. Truscott, *Photochem. Photobiol.*, **46**(5), 587 (1987).
28. H.H. Strain and J. Sherma, *J. Chem. Educ.*, **46**, 476 (1969).
29. M. Shiraki, M. Yoshiura, and K. Iriyama, *Chem. Lett.*, 103 (1978).
30. T. Braumann and L.H. Grimme, *Biochim. Biophys. Acta*, **637**, 8 (1981).
31. D.J.S. Birch and R.E. Imhof, *Anal. Instrum. (NY)*, **14**, 293 (1985).
32. D.L. Farrens and P.-S. Song, *Photochem. Photobiol.*, **54**, 313 (1991).
33. D.V. O'Conner and D. Phillips, "Time-Correlated Single Photon Counting," Academic Press, London, 1984.
34. S. Nonell, S.E. Braslavsky, and K. Schaffner, *Photochem. Photobiol.*, **51**, 551 (1990).
35. M.A.J. Rodgers, *Photochem. Photobiol.*, **37**, 99 (1983).

Received 24 January 1992